Self-consistent scattering analysis of $Al_{0.2}Ga_{0.8}N/AlN/GaN/AlN$ heterostructures grown on 6H-SiC substrates using photo-Hall effect measurements

Self-consistent scattering analysis of $Al_{0.2}Ga_{0.8}N$/AlN/GaN/AlN heterostructures grown on 6H-SiC substrates using photo-Hall effect measurements

S B Lisesivdin[1,5], E Arslan[2], M Kasap[1], S Ozcelik[1] and E Ozbay[2,3,4]

[1] Department of Physics, Faculty of Science and Arts, Gazi University, Teknikokullar, 06500 Ankara, Turkey

[2] Nanotechnology Research Center, Bilkent University, Bilkent, 06800 Ankara, Turkey

[3] Department of Physics, Bilkent University, Bilkent, 06800 Ankara, Turkey

[4] Department of Electrical and Electronics Engineering, Bilkent University, Bilkent, 06800 Ankara, Turkey

E-mail: sblisesivdin@gmail.com

Abstract

Hall effect measurements on undoped $Al_{0.2}Ga_{0.8}N$/AlN/GaN/AlN heterostructures grown on 6H-SiC substrates were carried out as a function of the temperature (30–300 K) and magnetic field (0–1.4 T). Measurements were carried out under dark and after-illumination conditions. After the dark measurements, the samples were illuminated with a blue light emitting diode for 30 min, and then the same measurements were carried out for the after-illumination condition. The magnetic field dependent Hall results were analyzed and the 2DEG contribution was found using the quantitative mobility spectrum analysis (QMSA) technique. A self-consistent scattering analysis between the dark and illuminated conditions was implemented. The importance of this implementation was to find an indirect way to locate more certain fit parameters, such as interface roughness parameters and the background impurity value, which cannot be found using dark measurement data alone.

1. Introduction

Over the last decade or so, gallium nitride (GaN) and its ternary alloys, such as aluminum gallium nitride (AlGaN) and indium gallium nitride (InGaN), have been the subject of intense research because of their successful applications in power electronics and optoelectronics [1–4]. With the advantage of high carrier mobilities, which are due to the formation of a two-dimensional electron gas (2DEG) at the heterojunction, AlGaN/GaN-based high electron mobility transistors (HEMTs) [5] are widely used in high power microwave applications and high temperature applications [6, 7]. Recently, Inoue *et al* claim to have

produced $Al_xGa_{1-x}N$ HEMTs on 6H-SiC substrates, which can operate above 475 K for 1×10^6 h [8]. However, the crystal quality is still a problem for GaN-based structures in the case of heteroepitaxial growth on foreign substrates because bulk GaN substrates are still expensive. The interface roughness of the heterojunction and the high impurity concentrations directly affect the mobility in GaN [9]. Most GaN material has an inherent, unintentional doping that is due to the growth process, which also affects the mobility. This unintentional doping causes n-type conductivity, which might have its origin in N vacancies [10] or impurities [11]. The effect of the interface roughness and impurities on 2DEG is strictly related to the performance of the AlGaN/GaN HEMTs. Therefore, the detailed characterization and studying the effects of the

---

[5] Author to whom any correspondence should be addressed.

interface roughness and impurities are rather important to achieve better device performances.

In the present study, we investigated the carrier mobility and density of a 2DEG as a function of temperature through the use of persistent photoconductivity (PPC). A persistent photo-induced increase in both 2DEG carrier mobility and density was found. The results of 2DEG carrier mobility and density were used to calculate the relevant scattering mechanisms, including background impurity and interface roughness scattering.

2. Experimental techniques

The $Al_xGa_{1-x}N/GaN$ ($x = 0.2$) heterostructures on (0001) on double-polished 2 inch 6H-SiC substrates were grown in a low pressure metal–organic chemical vapor deposition (MOCVD) reactor using trimethylgallium (TMGa), trimethylaluminum (TMAl), and ammonia as Ga, Al, and N precursors, respectively. The H_2 was used as a carrier gas during AlN and AlGaN growth. The buffer structure comprises a 15 nm thick, low temperature (650 °C) AlN nucleation layer, and a high temperature (1150 °C) 0.5 nm AlN template. A 2 μm nominally undoped GaN layer was grown on an AlN template layer, at 1050 °C, followed by a 1 nm thick high temperature AlN (1150 °C) interlayer.

The AlN interlayers are used to reduce the alloy disorder scattering by minimizing the wavefunction penetration from the 2DEG channel into the AlGaN barrier layer [12]. After the deposition of these layers, a 20 nm thick undoped $Al_{0.2}Ga_{0.8}N$ barrier layer was grown on an AlN interlayer at 1050 °C, and finally a 3 nm GaN cap layer was grown at the same temperature. At the beginning of the growth, the substrate was baked under H_2 ambient conditions at 1100 °C for 5 min in order to remove the native oxide. A schematic drawing of the structures is shown in figure 1.

For the Hall effect measurements by the van der Pauw method, square shaped (5 × 5 mm²) samples were prepared with four evaporated Ti/Al/Ni/Au triangular Ohmic contacts in the corners. Using gold wires and In soldering, the electrical contacts were made and their Ohmic behavior was confirmed by the current–voltage (I/V) characteristics. The measurements were performed at 12 temperature steps over a temperature range of 30–300 K using a Lake Shore Hall effect measurement system (HMS). At each temperature step, the Hall coefficient and resistivity were measured for the current directions, magnetic field polarization, and all of the possible contact configurations at 29 magnetic field steps between 0 and 1.4 T. The magnetic field dependent data were analyzed using the quantitative mobility spectrum analysis (QMSA) technique.

3. Results and discussion

Hall effect measurements of $Al_{0.2}Ga_{0.8}N/AlN/GaN/AlN$ heterostructures grown on 6H-SiC substrates were carried out as a function of the temperature (30–300 K) and magnetic field (0–1.4 T) in dark as well as illuminated conditions. Hall mobility and sheet carriers are shown in
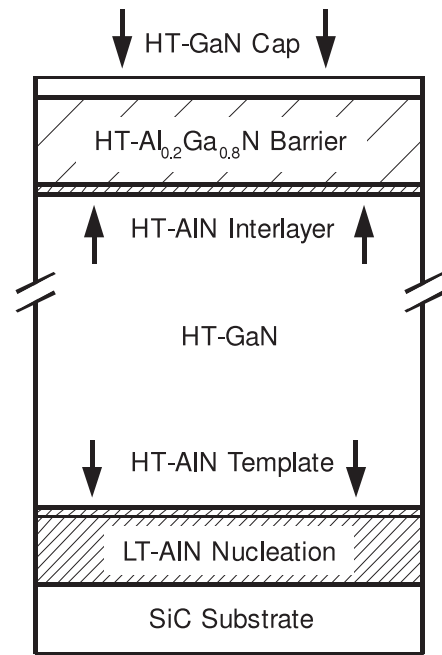

Figure 1. Layer structure of the studied samples.

figure 2. The dark measurements were carried out from 300 to 30 K (i). After 30 min of illumination with a blue light emitting diode (LED) (ii), a second measurement was performed in the dark from 30 to 300 K (iii). The mobility was independent of temperature under 100 K for both measurements. Sheet carrier density can be accepted as temperature independent in the studied range. These temperature dependences confirm the formation of the 2DEG in the studied samples. As can be seen in figure 2, mobility was enhanced at low temperatures and the sheet carrier density was significantly increased for the studied temperature range. The mobility in the after-illuminated state at 30 K reached a maximum value of approximately 5473 cm² V⁻¹ s⁻¹, which means a 43% enhancement, according to the dark value of 3831 cm² V⁻¹ s⁻¹. Moreover, the sheet carrier density value increased from 7.87×10^{12} cm⁻² to 1.23×10^{13} cm⁻² (a 56% increment) for the dark and after-illuminated states, respectively. Thus, the heterojunction device performance was dramatically improved by way of illumination.

QMSA is an effective technique for investigating the individual carrier species in a semiconductor. QMSA can extract the mobilities and sheet carrier densities of each species or conduction mechanisms by analyzing the magnetic field dependent Hall measurement data [13]. The QMSA technique has been applied successfully to various systems, including bulk InN [14], GaN epilayers [15], and AlGaN/GaN heterostructures [16]. However, the dimensionless product of lowest mobility and the highest field must be greater than unity to clearly identify additional carriers ($\mu_{min}B_{max} \gg 1$). In this study this condition seems to be barely fulfilled ($\mu_{min}B_{max} \leqslant 0.82$). As a lower bound value for mobility–field product, $\mu_{min}B_{max} = 0.5$ can be accepted as a limit [17]. Also in our previous study, we have successfully extracted different carriers in an AlGaN/GaN heterostructure grown on sapphire
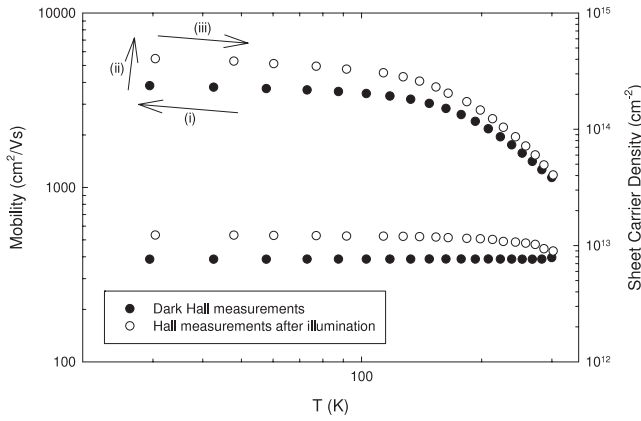
Figure 2. Measured mobility and sheet carrier densities of the dark measurements (filled circles) and measurements after illumination (empty circles). The arrows show the experiment sequence.
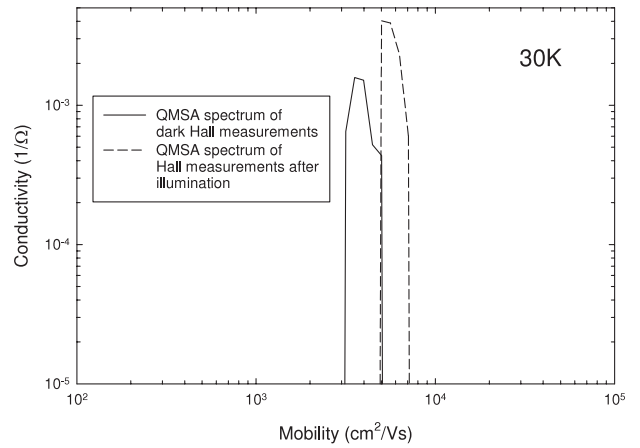

Figure 3. QMSA spectra for the studied samples at 30 K for dark measurements and the measurements after illumination.

even with slightly lower mobilities [18]. To expose the contributions of bulk conduction, we applied QMSA to the dark and after-illumination Hall data. In figure 3, the mobility spectra of the dark and after-illumination states are shown for 30 K. According to QMSA, only the 2DEG carrier exists even at high temperatures. In figure 3, mobility enhancement and an increase in conductivity of the 2DEG carrier can be seen clearly. Because the bulk carriers do not contribute to the total conductivity even at high temperatures, we accept that all of the conductivity is due to the 2DEG, and therefore we used the measured Hall data for further investigation. If QMSA could extract another carrier or channel, we had to use the extracted 2DEG carrier data. Therefore, QMSA or similar mobility spectrum analysis is important to extract the required data.

To investigate the mobility enhancement and increment in sheet carrier density in detail, 2DEG mobility analyses, by taking into consideration the most relevant scattering

mechanisms, were carried out using both dark and after-illumination Hall measurement data. In the present study, polar optical phonon scattering [19], acoustic phonon scattering [20], background impurity scattering [21], and interface roughness scattering [22] for 2D carriers were applied to the Hall data. These scattering mechanisms and their applications for AlGaN/GaN heterostructures in the dark were studied in detail in a previous study [23]. In the present study, the effect of the illumination was investigated. In addition, alloy disorder scattering [24] was not taken into account because of the AlN interlayers of the studied samples that were used to reduce the alloy disorder scattering by minimizing the wavefunction penetration from the two-dimensional electron gas (2DEG) channel into the AlGaN layer [12].

Mobility enhancement after illumination in semiconductor systems has been reported by several groups [25–30]. According to Li *et al*, mobility enhancement after illumination
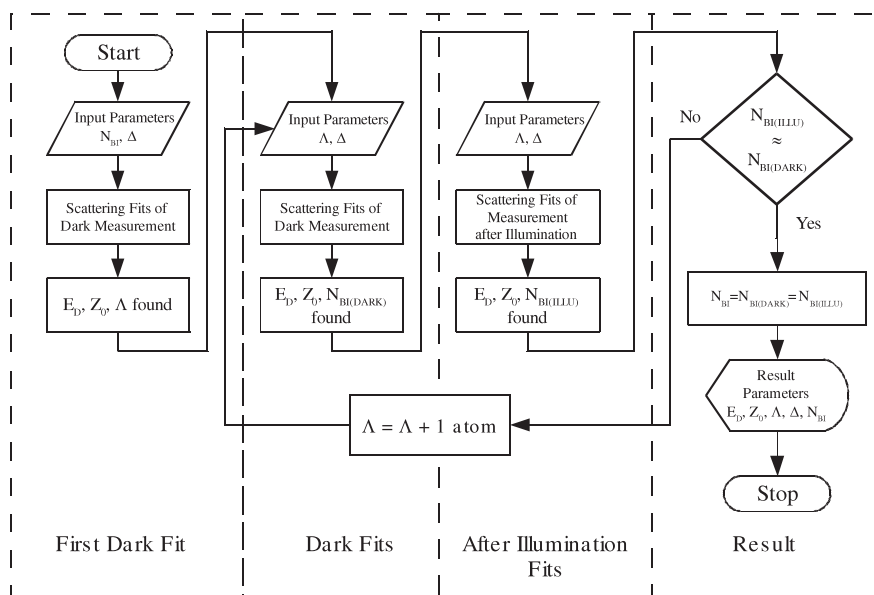

Figure 4. Flow chart of the self-consistent fit analyses between dark and after-illumination measurements.
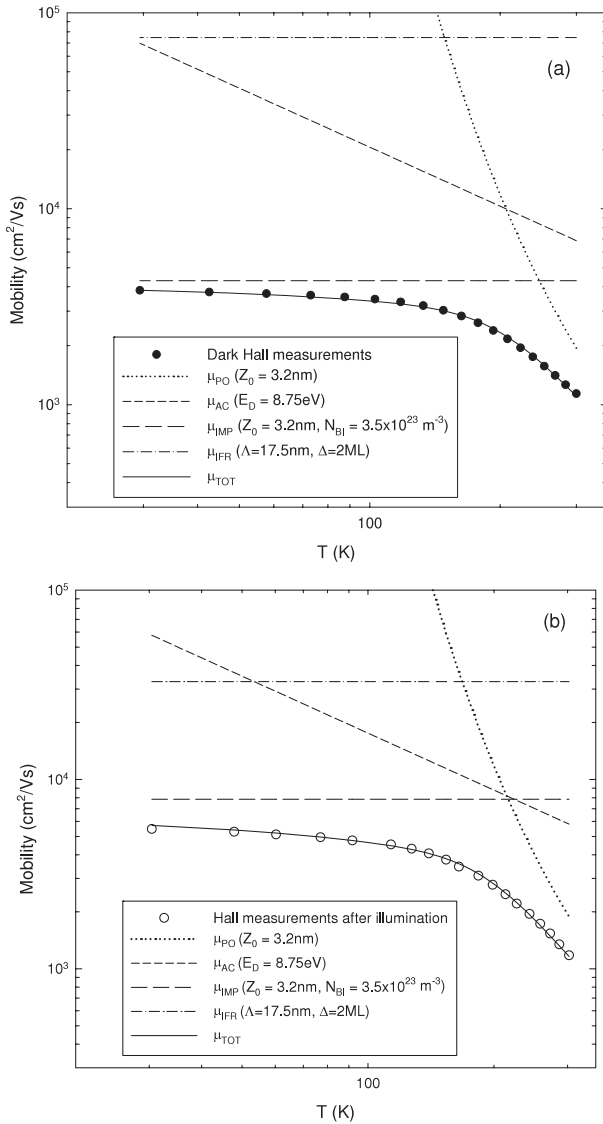
Figure 5. (a) Measured and calculated mobilities versus temperature using dark Hall measurements. (b) Measured and calculated mobilities versus temperature using the Hall measurements after illumination.

due to photoexcitation at a fixed temperature can be attributed to the increased electron mean energy with the increasing carrier density in the 2DEG channel, which results in a less efficient interaction of the 2DEG electrons with the ionized donor impurities as well as improved screening [25, 27]. An increase of the electron density in the 2DEG channel is primarily attributed to the transfer of photoexcited electrons from the deep-level impurities in the AlGaN epilayer [27]. Screening of the impurity related mobility enhancement was reported by Paesler and Quisser [29] and Hayne *et al* [30] in order to explain the all mobility change after illumination. In the present study, besides the background impurity scattering, interface roughness scattering is also effective at low temperatures. If the roughness of the interface can be accepted as independent of illumination, then the mobility enhancement at low temperatures can only be explained by background impurity scattering. To calculate the impurity

concentration, which can explain the mobility enhancement, we implement a self-consistent scattering fit process between the dark and illuminated conditions. In figure 4, the flow chart of the implementation is shown. Before the self-consistent fit process, scattering fits for the dark measurements were performed. Quantum well width (Z_0), deformation potential (E_D), and correlation length (Λ) values are found for an accepted lateral size value of $\Delta = 2$ ML and a beginning background impurity of $N_{BI} = 10^{23}$ m^{-3} [31]. Using these values as beginning input parameters, scattering fits for dark conditions were performed and a value for the background impurity is found ($N_{BI(DARK)}$). With the same input parameters, scattering fits for the illuminated condition were performed and a value of background impurity was found ($N_{BI(ILLU)}$). Because the mobility enhancement is only due to background impurity scattering, these impurity values must be equal. If not, the correlation length was increased by an amount of one atom length and the fits were performed again. This process was repeated unless $N_{BI(DARK)} \approx N_{BI(ILLU)}$.

In figure 5, mobility analysis results of the dark (a) and after illumination (b) are shown. Mobilitis limited by the individual scattering mechanisms, polar optical phonon, acoustic phonon, background impurity and dislocation scattering mechanisms, were calculated from the expressions given in our previous study [23]. Using Matthiessen's rule, the total mobility is then calculated as the combination of individual mobilities.

The fit of the scattering expressions to the dark mobility using the measured sheet carrier density at 0.5 T was carried out per the usual method. The calculated individual limiting mobilities and total mobility are shown in figure 5(a). It can be seen in the figure that the mobility fits quite well to the data with the fit parameters of well width $Z_0 = 3.2$ nm, deformation potential constant $E_D = 8.75$ eV, number of impurities $N_{BI} = 3.5 \times 10^{23}$ m^{-3} and correlation length $\Lambda = 17.5$ nm for the accepted lateral size of $\Delta = 2$ ML.

The calculated individual limiting mobilities and total mobility of the illuminated situation are shown in figure 5(b) by using the same fit parameters as for the dark situation. Because the fit parameters of well width and deformation potential do not change in the self-consistent fit process, we can assume that the phonon scatterings are not related to the increase in mobility. Because we assumed that the interface roughness was not altered by the illumination and the all mobility enhancement was caused by activated impurities, the parameters of interface roughness scattering and background impurity scattering were also unchanged.

In figure 6, the sheet carrier density dependent theoretical calculations of the mobilities of acoustic phonon scattering, background impurity scattering, and interface roughness scatterings are shown for 30 K. With an increase in sheet carrier density, the background impurity scattering should be less effective. While for the sheet carrier density values $n_S < 1.7 \times 10^{13}$ cm^{-2} the background impurity scattering is effective, above this value interface roughness scattering becomes more effective than background impurity scattering. In addition, acoustic phonon scattering is less effective for all sheet carrier density values. It is clearly seen that background impurity scattering is strongly effective for the studied samples.
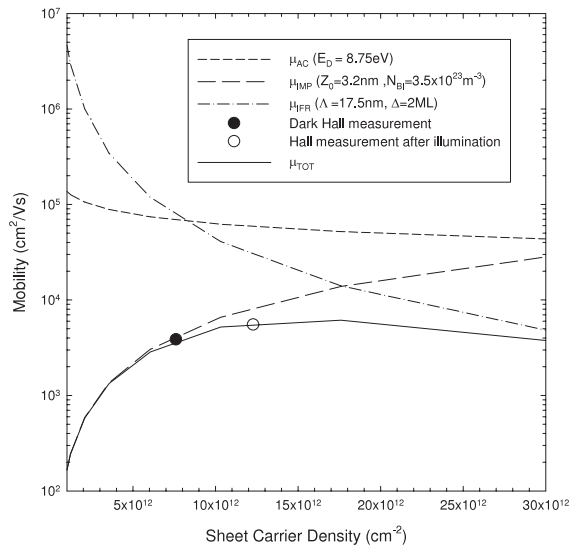
Figure 6. 2DEG mobility versus the sheet carrier density at 30 K. Lines represent the result of the theoretical calculations of mobilities at 30 K limited by alloy, acoustic phonons, background impurities and interface roughness. Dark and after-illumination measurement results at 30 K are shown with filled and empty symbols, respectively.

4. Conclusion

Hall effect measurements on undoped $Al_{0.2}Ga_{0.8}N/AlN/GaN/AlN$ heterostructures grown on 6H-SiC substrates were carried out as a function of the temperature (30–300 K) and magnetic field (0–1.4 T). Measurements were carried out firstly under dark conditions. After the dark measurements, the samples were illuminated with a blue LED for 30 min, and then the same measurements were carried out for the after-illumination conditions. The magnetic field dependent Hall results were analyzed using QMSA. Because the bulk carriers do not contribute much to the total conductivity, even at high temperatures, all of the conductivity is accepted to be due to 2DEG, and therefore the measured Hall data are used for the scattering analyses. The scattering analyses for the dark and after-illumination measurements showed that illumination does not influence the phonon related scattering mechanisms. A self-consistent scattering analysis between the dark and illuminated conditions was implemented using the fit constants of phonon related scattering mechanisms, and the acceptance of interface roughness was independent of illumination. With this implementation, the background impurity related mobility enhancement is explained rather well. The importance of this implementation is to find an indirect way to locate more certain interface roughness parameters and background impurity values, which cannot be located by using dark measurement data alone. In addition, the sheet carrier density dependent theoretical calculations of the mobilities of acoustic phonon, background impurity, and interface roughness scatterings were all investigated. The strong influence of the background impurity scattering is shown for the studied samples.

References

[1] Morkoc H, Strite S, Gao G B, Lin M E, Sverdlov B and Burns M 1994 *J. Appl. Phys.* **76** 1363
[2] Khan M A, Shur M S, Kuznia J N, Chen Q, Burn J and Schaff W 1995 *Appl. Phys. Lett.* **66** 1083
[3] Koide N, Kato H, Sassa M, Yamasaki S, Manabe K, Hashimoto M, Amano H, Hiramatsu K and Akasaki I 1991 *J. Cryst. Growth* **115** 636
[4] Nakamura S, Senoh M, Nagahama S, Iwasa N, Yamada T, Matsushita T, Kiyoku H, Sugimoto Y, Kozaki T, Umemoto H, Sano M and Chocho K 1998 *Appl. Phys. Lett.* **72** 211
[5] Ambacher O, Foutz B, Smart J, Shealy J R, Weimann N G, Chu K, Murphy M, Sierakowski A J, Schaff W J, Eastman L F, Dimitrov R, Mitchell A and Stutzmann M 2000 *J. Appl. Phys.* **87** 334
[6] Khan M A, Chen Q, Yang J W, Shur M S, Dermott B T and Higgins J A 1996 *IEEE Electron Device Lett.* **17** 325
[7] Sheppard S T, Doverspike K, Pribble W L, Allen S T, Palmour J W, Kehias L T and Jenkins T J 1999 *IEEE Trans. Electron Device Lett.* **20** 161
[8] Inoue Y, Masuda S, Kanamura M, Ohki T, Makiyama K, Okamoto N, Imanishi K, Kikkawa T, Hara N, Shigematsu H and Joshin K 2007 *Microwave Symp., IEEE/MTT-S Int.* p 639
[9] Gokden S 2004 *Physica* E **23** 114
[10] Wetzel C, Walukiewicz W, Haller E, Ager J, Grzegory I, Porowski S and Suski T 1996 *Phys. Rev.* B **53** 1322
[11] Neugebauer J and Van de Walle C 1996 *Appl. Phys. Lett.* **69** 503
[12] Lisesivdin S B, Yildiz A and Kasap M 2007 *Optoelectron. Adv. Mater. Rapid Commun.* **1** 467
[13] Antoszewski J, Faraone L, Vurgaftman I, Meyer J R and Hoffman C A 2004 *J. Electron Mater.* **33** 673
[14] Swartz C H, Tomkins R P, Giles N C, Myers T H, Lu H, Schaff W J and Eastman L F 2004 *J. Cryst. Growth* **269** 29
[15] Swartz C H, Tomkins R P, Myers T H, Look D C and Sizelove J R 2005 *J. Electron. Mater.* **33** 412
[16] Biyikli N, Xie J, Moon Y-T, Yun F, Stefanita C-G, Bandyopadhyay S, Morkoç H, Vurgaftman I and Meyer J R 2006 *Appl. Phys. Lett.* **88** 142106
[17] Vurgaftman I, Meyer J R, Hoffman C A, Redfern D, Antoszewski J, Faraone L and Lindemuth J R 1998 *J. Appl. Phys.* **84** 4966
[18] Lisesivdin S B, Yildiz A, Acar S, Kasap M, Ozcelik S and Ozbay E 2007 *Appl. Phys. Lett.* **91** 102113
[19] Ridley B K 1982 *J. Phys. C: Solid State Phys.* **15** 5899
[20] Ridley B K, Foutz B E and Eastman L F 1999 *Phys. Rev.* B **61** 16862
[21] Hess K 1979 *Appl. Phys. Lett.* **35** 484
[22] Zanato D, Gokden S, Balkan N, Ridley B K and Schaff W J 2004 *Semicond. Sci. Technol.* **19** 427
[23] Lisesivdin S B, Acar S, Kasap M, Ozcelik S, Gokden S and Ozbay E 2007 *Semicond. Sci. Technol.* **22** 543
[24] Kearney M J and Horrell A I 1998 *Semicond. Sci. Technol.* **13** 174
[25] Li J Z, Lin J Y, Jiang H X, Khan M A and Chen Q 1997 *J. Appl. Phys.* **82** 1227

[26] Babinski A, Li G and Jagadish C 1997 *Appl. Phys. Lett.* **71** 1664

[27] Li J Z, Lin J Y, Jiang H X, Khan M A and Chen Q 1997 *J. Vac. Sci. Technol.* **15** 1117

[28] Wang W, Chua S J and Li G 2000 *J. Electron. Mater.* **29** 27

[29] Paesler M A and Queisser H J 1978 *Phys. Rev.* B **17** 2625

[30] Hayne M, Usher A, Harris J J, Moshchalkov V V and Foxon C T 1998 *Phys. Rev.* B **57** 14813

[31] Zhang G Y, Tong Y Z, Yang Z J, Jin S X, Li J and Gan Z Z 1997 *Appl. Phys. Lett.* **71** 3376